Available online at www.sciencedirect.com

ScienceDirect

journal homepage: www.JournalofSurgicalResearch.com

Shockwave therapy improves anterior cruciate ligament reconstruction

Ching-Jen Wang, MD,[a] *Jih-Yang Ko, MD,*[a] *Wen-Yi Chou, MD,*[a] *Shan-Ling Hsu, MD,*[a] *Sheung-Fat Ko, MD,*[b] *Chung-Cheng Huang, MD,*[b,*] *and Hsueh-Wen Chang, PhD*[c]

[a] *Center of Shockwave Medicine and Tissue Engineering, Department of Orthopedic Surgery, Chang Gung Memorial Hospital/Kaohsiung Medical Center, Chang Gung University College of Medicine, Taiwan*

[b] *Department of Radiology, Chang Gung Memorial Hospital/Kaohsiung Medical Center, Chang Gung University College of Medicine, Taiwan*

[c] *Department of Biological Sciences, Center for Research in Medical Science and Technology, National Sun Yat-Sen University, Kaohsiung, Taiwan*

ARTICLE INFO

Article history:
Received 24 June 2013
Received in revised form
1 August 2013
Accepted 20 August 2013
Available online 31 January 2014

Keywords:
ACL
Shockwave
Tendon–bone healing

ABSTRACT

Background: Shockwave was shown to enhance the healing of anterior cruciate ligament (ACL) reconstruction in rabbits. This study evaluated the effect of extracorporeal shockwave therapy (ESWT) on ACL reconstruction in human subjects. We hypothesized that ESWT may improve human ACL reconstruction.

Methods: Fifty-three patients were randomized into two groups with 26 patients in ESWT group and 27 patients in control group. The ESWT group underwent single-bundle hamstring autograft ACL reconstruction and received ESWT immediately after surgery. The control group underwent ACL surgery without ESWT. Both groups received the same rehabilitation postoperatively. The evaluations included Lysholm score, IKDC score and KT-1000, radiograph, bone mineral density, and magnetic resonance imaging.

Results: ESWT group showed significantly better Lysholm score than control group at 1 and 2 y postoperatively ($P < 0.001$ and 0.001, respectively). No significant difference was noted in IKDC score between the two groups ($P = 0.080$ and 0.076, respectively). The KT-1000 values were significantly better in ESWT group than control group at 2 y postoperatively ($P = 0.027$). The tibia tunnel on X-ray was significantly smaller in ESWT group compared with control group at 2 y ($P = 0.018$). The bone mineral density values showed no discernable difference between the two groups at 6 mo and 2 y ($P = 0.522$ and 0.984, respectively). On magnetic resonance imaging, ESWT group showed significant decrease in tibia tunnel enlargement at 6 mo and 2 y compared with the control group ($P = 0.024$ and <0.001, respectively).

Conclusions: ESWT significantly improves the subjective Lysholm score and decreases the middle 1/3 tibia tunnel enlargement after single hamstring autograft ACL reconstruction.

* *Corresponding author*. Department of Diagnostic Radiology, Chang Gung Memorial Hospital/Kaohsiung Medical Center, 123 Ta-Pei Road, Niao Sung District, Kaohsiung, Taiwan 833. Tel.: +88 67 733 5279; fax: +88 67 733 5515.
E-mail address: w281211@adm.cgmh.org.tw (C.-C. Huang).

0022-4804/$ – see front matter © 2014 Elsevier Inc. All rights reserved.
http://dx.doi.org/10.1016/j.jss.2014.01.050

1. Introduction

Anterior cruciate ligament (ACL) reconstruction is usually performed by the transfer of a free tendon graft into a bone tunnel. The functional outcome of ligament reconstruction relies on the firm healing of tendon to bone in the bone tunnel. The phenomenon of ligamentization after free autograft ACL reconstruction remains controversial [1]. Previous studies showed conflicting results [2–9]. Some studies demonstrated the phenomenon of ligamentization after implantation of tendon autograft into a bone tunnel [2,5,7–9]. However, other studies showed the opposite results and concluded that metaphyseal bone and tendon do not heal together [3,4,6].

Many factors may influence the healing of tendon to bone in ACL surgery. Some studies demonstrated that bone morphogenic protein is effective in promoting bone formation and the healing of tendon to bone in a bone tunnel [10–13]. Other studies attempted to improve the healing of tendon to bone with different modalities including periosteum augmentation, calcium phosphate cement, tricalcium phosphate, calcium phosphate–hybridized tendon, granulocyte colony–stimulating factor, magnesium-based adhesive, hyperbaric oxygen therapy, and gene transfer [14–21]. Some reported limited success, but none showed consistent results. In animal experiment, extracorporeal shockwave therapy (ESWT) was shown to induce the ingrowth of neovascularization and promote tissue repair [22–24]. Prior studies demonstrated that ESWT is effective in promoting tendon–bone healing in bone tunnel after ACL reconstruction in a rabbit model [23].

In clinical setting, bone tunnel enlargement on radiograph and magnetic resonance imaging (MRI) are often used as the evaluation parameters after ACL reconstruction. [25] Many factors may affect the bone tunnel enlargement including the fixation type and the location. The implication of bone tunnel enlargement after ACL reconstruction and subsequent mechanical instability is still debated [25–30]. Some authors concluded that bone tunnel enlargement is the main contributory factor that leads to laxity of ACL autograft [25,29,30]. Many studies addressed different approaches to prevent or reduce the risk of bone tunnel enlargement after ACL reconstruction including adding autograft or allograft bone plugs, use of biocomposite interference screw fixation, and the use of aperture fixation. However, there is no consensus on the best method [31–34]. The purpose of this prospective study was to evaluate the effect of ESWT on the functional outcome and the decrease of tibia tunnel enlargement after hamstring autograft ACL reconstruction. We hypothesized that ESWT may improve the functional outcome and decrease the tibia tunnel enlargement in hamstring autograft ACL reconstruction.

2. Materials and methods

The Institutional Review Board approved this study. Each patient was required to sign an informed consent before participation in the study. The inclusion criteria included patients with an ACL-deficiency knee undergoing primary ACL reconstruction. The exclusion criteria included revision ACL surgery, previous knee surgery, and knees with multiple ligament injury. Fifty-three patients with 53 knees were included in the study. Patients were randomly divided into two groups using the computer-generated block labels. Twenty-six patients (26 knees) with odd numbers were assigned to the ESWT group, whereas 27 patients (27 knees) with even numbers were assigned to the control group. The flow chart of patient recruitment is shown in Figure 1. The demographic characteristics are shown in Table 1. Patients in the ESWT group underwent arthroscopic single-bundle semitendinosus autograft ACL reconstruction and received ESWT immediately after surgery. Patients in the control group underwent single-bundle semitendinosus autograft ACL reconstruction, but no ESWT after surgery.

2.1. ACL reconstruction

With patient under general or spinal anesthesia, the affected leg was draped in sterile fashion. A complete arthroscopic examination of the knee was performed. The associated injuries including meniscal tears and chondral lesions were identified. The procedure was concomitantly performed for associated meniscal and chondral lesions. Meniscal tears were noted in eight knees (31%) of the ESWT group and seven knees (26%) of the control group. Meniscus repair was performed in four cases each of the ESWT and the control groups, whereas partial meniscectomy was done in four and three cases of the ESWT group and the control group, respectively. Chondral defects were seen in four cases in each group, and the small lesions (<1.0 cm) were managed with debridement. During ACL reconstruction, the ACL stump was partially debrided. The locations of the femoral tunnel on the lateral femoral condyle and the tibia tunnel in tibia eminence were verified anatomically using the ACL footprints as the landmarks under arthroscopy. A 25-mm long incision was made on the anteromedial aspect of the proximal tibia. The semitendinosus tendon was harvested with a tendon stripper. The tendon graft was folded in either tripled or quadrupled fashion depending on the graft length and was sutured into a graft construct. The average graft size was 8 mm in diameter × 85 mm in length. The graft was pretensioned with 15 lb on tension device for 15 min before implantation. The ACUFEX instruments (Smith & Nephew, Andover, MA) were used in ACL reconstruction. The guide pin was inserted from either the anteromedial or extended medial portal into the knee joint. The footprint on the bony ridge of the lateral femoral condyle was referenced for femoral tunnel location. The femoral tunnel was created with a graft size matched reamer to a depth of 25 mm. Similarly, the tibia tunnel in tibia eminence was created with graft size–matched reamer. The tendon graft was delivered from tibia tunnel into the knee joint and then the femoral tunnel. Both ends of the graft were secured with bio-screws (MiTek products, Ethicon Inc, Johnson & Johnson Company, Marlborough, MA) with the knee at 20°–30° of flexion. The femoral side was fixed first, and the tibia fixation was done afterward while the graft tension was maintained distally. The bio-screws were either the same size or one size smaller than the bone tunnel depending on the bone quality assessed during tunnel drilling.

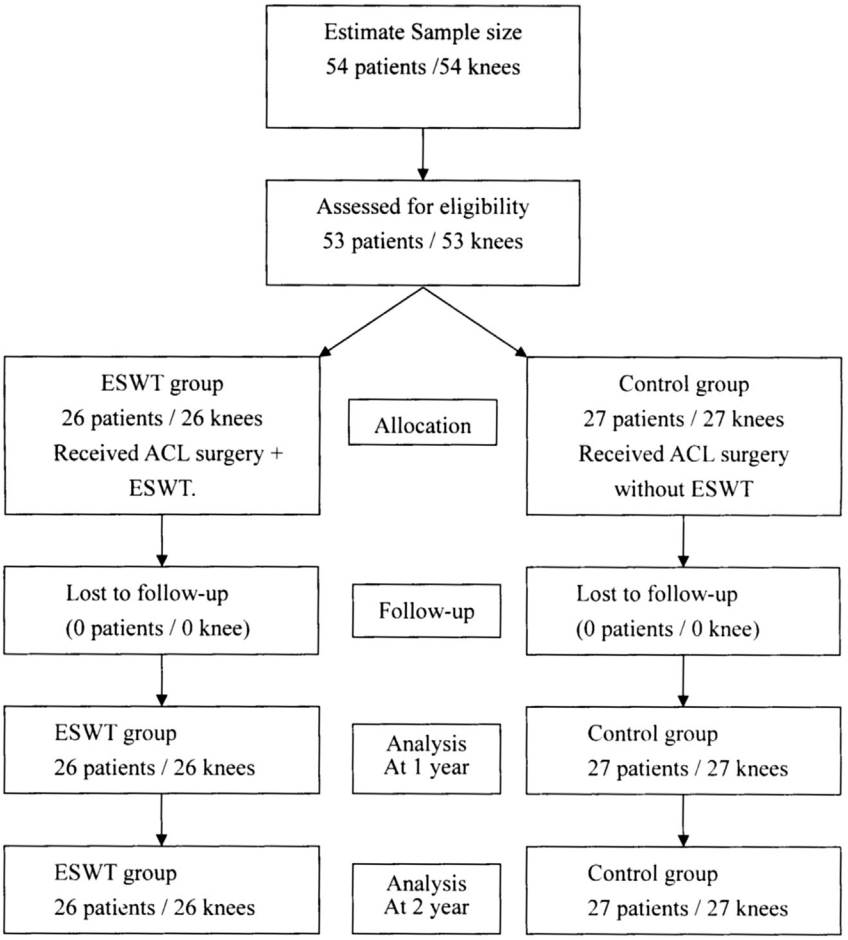

Fig. 1 – The flow chart of patient recruitment.

2.2. *ESWT application*

Patients in the ESWT group also received ESWT immediately after ACL surgery under the same anesthesia. The source of shockwave was from an OssaTron (High Medical Technology, Lengwil, Switzerland. It is now SANUWAVE, Alpharetta, GA). The surgical wounds were covered with sterile cellulose barrier, and ultrasound gel was applied to the skin in contact with the shockwave tube. The shockwave was focused at the middle third of the tibia tunnel in anterior–posterior (AP) and lateral views, and the depth of treatment was verified by adjusting the height of the table until the two ring markers of

Table 1 – Patient demographic characteristics.

	ESWT group ($N = 26$)	Control group ($N = 27$)	P
Age (y)*	28.3 ± 7.4 (15–45)	27.7 ± 7.7 (17–53)	0.858
Males/females	21/5	21/6	0.788
Right knee/left knee	15/11	14/13	0.669
Duration of symptoms (mo)*	21.4 ± 22.5 (1–72)	15.4 ± 21.9 (1–84)	0.167
Mechanism of injury			
Baseball injury	11/26	16/27	0.217
Traffic accident	8/26	6/27	0.480
Falling accident	5/26	1/27	0.075
Other	2/26	4/27	0.413
Meniscus injury†	8/26 (31%)	7/27 (26%)	0.810
Chondral injury	4/26 (15%)	4/27 (15%)	0.954
Length of follow-up (mo)*	41.2 ± 12.9 (24–55)	41.0 ± 13.5 (24–55)	0.613

*Mean ± SD (range); ESWT: extracorporeal shockwave therapy; the numeric data between the ESWT and control groups are analyzed with Mann–Whitney U-tests, and the nominal data are analyzed with Chi-square or Fisher exact tests.
†Meniscus repairs in four cases each and partial meniscectomy in four and three cases of the ESWT group and the control group, respectively.

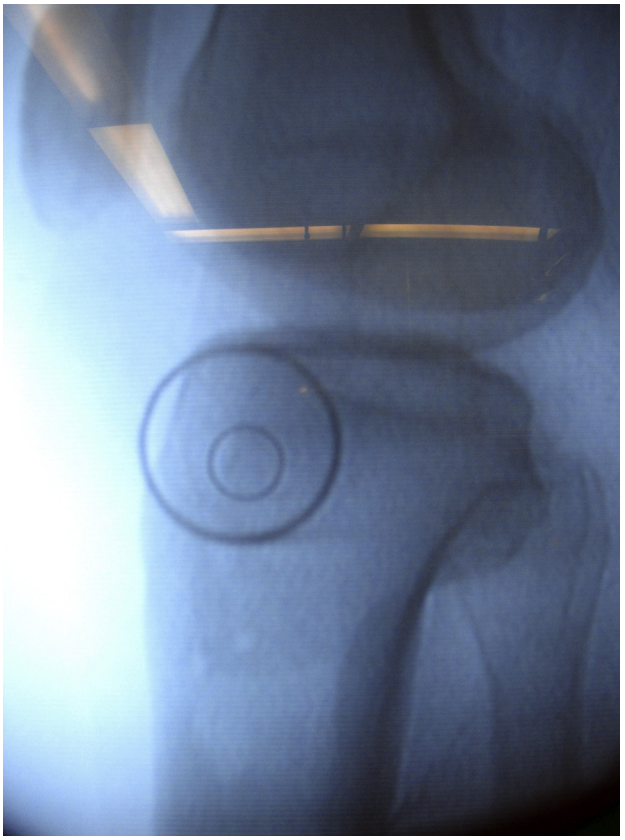

Fig. 2 – The C-arm imaging of the proximal tibia in lateral projection shows the depth of ESWT application. (Color version of figure is available online.)

the device synchronized on C-arm imaging (Fig. 2). Application of 1500 impulses of ESWT at 20 kV (equivalent to 0.298 mJ/mm^2 energy flux density) was administered to the middle third of the tibia tunnel in a single session. The dosage so chosen in this study was based on the results of another study [35]. For the study purposes, ESWT was applied only to the tibia tunnel. Immediately after ESWT application, the local area was checked for swelling, ecchymosis, hematoma, and so forth. Patients in the control group received no ESWT after ACL reconstruction.

Postoperatively, all patients received the same rehabilitation program that included crutch walking with partial weight bearing, range of knee motion, and quadriceps and hamstring exercises for 3–6 wk. Patients were discharged when they were capable of independent crutch walking and continued outpatient physical therapy. Full weight bearing was permitted after 6 wk.

2.3. *Clinical assessment and image study*

The evaluations included clinical assessment, radiograph, bone mineral density (BMD), and MRI of the affected knee. Clinical assessments including Lysholm functional score, IKDC subjective score, and AP laxity of the knee were performed before treatment and at each follow-up visit. The AP knee laxity was evaluated with physical examination and KT-1000 arthrometer with 20-lb pull. The values of KT-1000 arthrometer represent the absolute values on the same knee before and after surgery. Radiographs of the knee in anteroposterior and lateral views were obtained at 1 wk after treatment and at each follow-up visit. Radiographs were used to evaluate the bony appearance and the changes of the tibia bone tunnel size at proximal 1/3, middle 1/3, and distal 1/3 on anteroposterior and lateral views. BMD in the region of interest around the tibia tunnel was performed at 1 wk (T0), 6 (T6 mo), and 24 mo (T24 mo) after treatment using dual energy x-ray absorptiometry. The BMD was used to assess the changes in bone density of the proximal tibia and distal femur.

MRI of the knee was performed at T0, T6 mo, and T24 mo after treatment. The imaging study was carried out using a 3.0 T MR system (Signa Excite HD, General Electric Medical Systems, Milwaukee, WI). Cyst formation or fluid collection in or around the tibia tunnel, if any, was documented. The baseline MRI protocol included proton-weighted coronal and sagittal, proton-weighted oblique coronal and oblique sagittal along the tibia tunnel axis, T1-weighted oblique axial, and fat-saturated proton-weighted oblique axial perpendicular to the long axis of tibia tunnel pulse sequences. The signal change of autograft, autograft–bone marrow interface, diameter, and area of the tibia tunnel on the MRI were recorded. The oblique axial fat-suppressed proton-weighted images were used to assess the autograft cross-sectional areas and autograft-bone interface (Fig. 3A). The middle portions of upper, middle, and lower third tibia tunnel images were captured using the PACS system and then analyzed in the Image-Pro Plus software (Media Cybernetics, Silver Spring, Maryland) [27,30]. The color threshold level within the software program was set to encompass the low-signal tendon autograft in the tibia tunnel for calculating autograft area. The corresponding screw area in tibia tunnel was measured digitally using a computer-generated best-fit circle (Fig. 3B) [27,30,36,37]. To minimize the measurement error due to variance of the corresponding cross-sectional areas taken by sequential MRI examinations, we used autograft–screw area ratio (ASR = autograft area over screw area) to represent cross-sectional area of the autograft. The ratios of ASR at T6 mo (ASRT6) divided by ASR at T0 (ASRT0), ASR at T24 mo (ASRT24) divided by ASRT0, and ASRT24 divided by ASRT6 were measured to represent the ratios of decreasing low-signal autograft between each two time sets. The healing of autograft was defined as loss of low-signal autograft due to incorporation of the graft into the surrounding bone marrow on MRI images. Therefore, the integration ratio of the autograft at T6 mo or T24 mo could be obtained from the following formulas: integration ratio at T6 mo = 1 – (ASRT6/ASRT0), at T24 mo = 1 – (ASRT24/ASRT0), and at T6 mo to T24 mo = 1 – (ASRT24/ASRT6). The integration ratios of the upper, middle, and lower third of the tibia tunnel were measured separately, and the mean of these three integration ratios was used to evaluate the effect of ESWT on tendon–bone healing.

The AP and medial–lateral (ML) diameters of the upper, middle, and lower third of the tibia tunnel were recorded using the oblique axial T1-weighted images (Fig. 4A and B). The corresponding area of the tibia tunnel was calculated using the area of ellipse as $\pi \times$ half AP diameter $\times$ half ML

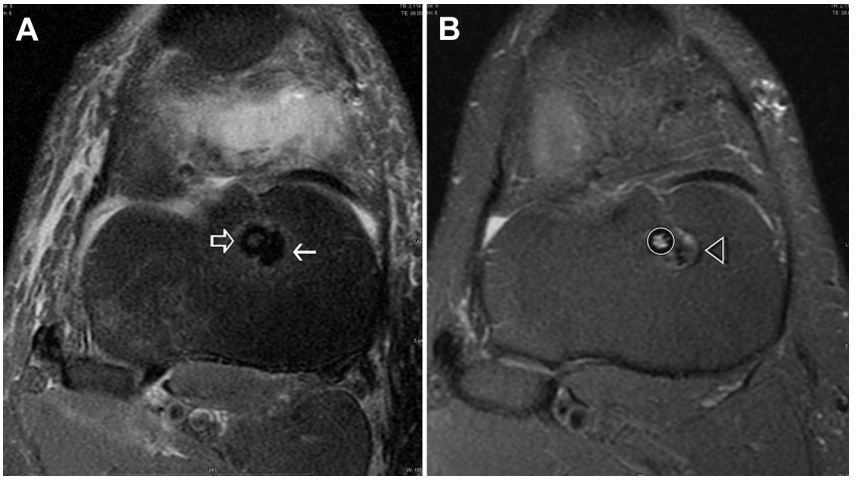

Fig. 3 – MRI of a 31-y-old male patient of the ESWT group. (A) The fat-suppressed oblique axial proton-weighted MR image exhibits hypointense autograft (arrow) and screw (open arrow) in the upper third of the tibia tunnel immediately after surgery. Also noted is the edematous change of subcutis and Hoffa's fat pad. (B) Six months after ESWT treatment integration of the autograft with surrounding bone marrow of the tibia tunnel (open arrowhead) is evident. The best-fit circle of the screw is used for area calculations.

diameter. The enlargement ratios of AP diameter, ML diameter, and area of the tibia tunnel were measured by the values at T6 mo/values at T0, T24 mo/values at T0, and T24 mo/values at T6 mo. The mean enlargement ratio of upper, middle, and lower third of the tibia tunnel was used to analyze tunnel enlargement. Two radiologists blinded to the study design jointly performed the MRI interpretation.

2.4. *Statistical analysis*

A power analysis revealed that for a power of 80% and $\alpha = 0.05$, a sample size of 27 patients in each group is required to achieve significance with a mean difference 6.5, standard deviation 4.5 on Lysholm score at 1 y after treatment. The data before and after treatment at 6 mo and 1 and 2 y within the same group were compared by Friedman test. If the Friedman test showed significant difference, Wilcoxon signed rank tests with Bonferroni correction were used to analyze the differences between each repeated measurement. The nominal and numeric data between the ESWT group and the control group were compared statistically with Chi-square and Mann–Whitney *U*-tests respectively. The statistical significance was set at $P < 0.05$.

3. Results

The patient demographic characteristics showed no significant differences between the two groups (Table 1). The Lysholm functional score, IKDC subjective score, and ligament laxity of the knee are summarized in Table 2. Compared with those data before treatment, significant improvements in functional score, IKDC subjective score, and ligament laxity of the knee were noted in both groups at 1 and 2 y after treatment (all $P < 0.05$). However, the ESWT group showed

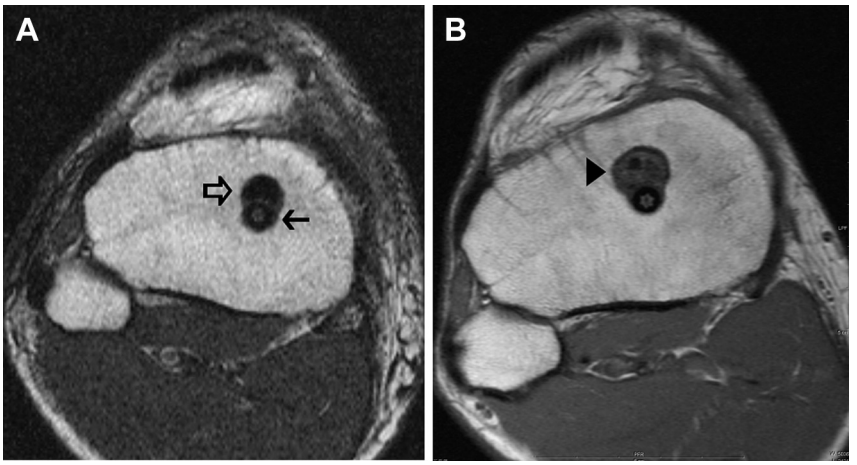

Fig. 4 – MRI of a 27-y-old male patient of the control group. (A) Oblique axial T1-weighted axial MR image depicts ACL autograft (open arrow) and screw (arrow) in the tibia tunnel immediately after surgery. (B) Apparent enlargement of the tibia tunnel (arrowhead) is noted 6 mo later.

Table 2 – Lysholm function score, IKDC subjective score, and KT-1000 arthrometer for AP laxity of the knee.

Evaluation N = 26 ESWT N = 27 Control	Before Tx	At 1 y	At 2 y	P*
Lysholm score				
ESWT group	50.7 ± 14.4 (26–70)[a]	94.0 ± 4.9 (94–99)[b]	95.0 ± 4.6 (95–100)[b]	<0.001
Control group	46.2 ± 16.7 (21–75)[a]	87.3 ± 6.4 (66–99)[b]	89.0 ± 7.9 (66–100)[b]	<0.001
P†	0.209	<0.001	0.001	
IKDC score				
ESWT group	23.5 ± 8.0 (6.3–37.3)[a]	60.7 ± 4.5 (51.3–68.3)[b]	62.1 ± 4.2 (58.3–71.3)[b]	<0.001
Control group	21.0 ± 9.2 (2.3–37.3)[a]	56.2 ± 6.8 (32.3–64.3)[b]	58.8 ± 8.1 (32.3–71.3)[b]	<0.001
P†	0.285	0.080	0.076	
KT-1000 (in mm)				
ESWT group	8.2 ± 2.4 (5–13)[a]	3.0 ± 1.3 (0–5)[b]	2.4 ± 1.0 (1–4)[b]	<0.001
Control group	8.6 ± 2.0 (9–13)[a]	3.6 ± 1.5 (1–7)[b]	3.4 ± 1.4 (1–6)[b]	<0.001
P†	0.516	0.188	0.027	

The data are expressed in mean ± SD (range). Means with different letters ([a] or [b]) are significantly different ($P < 0.05$, Wilcoxon Signed Ranks Test for paired data with Bonferroni correction).
* P: by Friedman test.
† P: compared between ESWT group and control group by Mann–Whitney U-tests.

significantly better Lysholm functional score and AP laxity of the knee compared with the control group at 2 y ($P = 0.001$ and 0.027, respectively), but the IKDC subjective score was not different between the two groups ($P = 0.076$). The tibia tunnel size on radiograph at T0, T12 mo, and T24 mo and BMD values at T0, T6 mo, and T24 mo are shown in Table 3. The size of the tibia tunnel showed a trend of increase at T12 m and a decrease at T24 mo in both groups. Nevertheless, the size at the middle 1/3 of the tibia tunnel was significantly smaller in the ESWT group compared with the control group ($P = 0.018$) suggesting that the changes in tibia tunnel size were more pronounced at the middle 1/3 where ESWT was applied. The changes in BMD values of the proximal tibia revealed no discernible difference between the two groups ($P = 0.522$ and 0.984, respectively).

On MRI, the autograft appeared homogeneous and hypointense in the tibia tunnel at T0 that was similar to the signal characteristics of the native harvest tissue (Fig. 3A). Partial loss of hypointense autograft appearance and gradual healing into the surrounding bone marrow of the tibia tunnel were observed at T6 mo and T24 mo in both the groups. The mean ASRs and integration ratios of the ACL autograft in the tibia tunnel at T0, T6 mo and T24 mo are summarized in the Table 4. Overall, gradual reduction of the autograft area with time was noted in both groups. The mean ASRs in the ESWT group at T6 mo and T24 mo were significantly smaller than those in the control group ($P = 0.002$ and <0.001, respectively). Compared to the autograft at T0, the mean integration ratios at T6 mo and T24 mo in the ESWT group were significantly better than those in the control group ($P = 0.001$ and <0.001).

Table 3 – Tibia tunnel size on radiographs and BMD around tibia tunnel.

Tibia tunnel (in mm) N = 26, ESWT N = 27 Control	At T0	At T12 mo	At T24 mo	P*
ESWT group				
Proximal 1/3	10.8 ± 1.6 (7.1–12.8)[a]	10.9 ± 1.7 (7.6–13.7)[a]	10.7 ± 1.4 (8.5–13.1)[a]	0.307
Middle 1/3	10.7 ± 1.8 (6.7–13.8)[a]	10.6 ± 1.7 (7.6–13.5)[a]	8.8 ± 0.9 (7.1–10.3)[b]	0.046
Distal 1/3	9.9 ± 2.3 (4.8–14.5)[a]	9.7 ± 2.0 (5.8–13.0)[a]	9.2 ± 0.8 (7.8–1.5)[a]	0.706
Control group				
Proximal 1/3	10.3 ± 1.6 (7.4–14.8)[a]	10.1 ± 2.2 (6.3–15.2)[a]	10.3 ± 1.9 (10.4–13.1)[a]	0.223
P†	0.141	0.149	0.620	
Middle 1/3	10.9 ± 2.5 (7.4–18.9)[a]	10.1 ± 2.1 (6.7–14.1)[a]	10.1 ± 1.5 (9.7–12.4)[a]	0.683
P†	0.875	0.424	0.018	
Distal 1/3	9.7 ± 1.5 (7.1–14.5)[a]	9.6 ± 2.1 (5.9–12.8)[a]	9.4 ± 1.5 (7.4–12.5)[a]	0.611
P†	0.925	0.964	0.577	
BMD (g/cm^2)	At T0	At T6 mo	At T24 mo	
ESWT group	0.89 ± 0.22 (0.56–1.31)[a]	0.81 ± 0.17 (0.34–0.11)[a]	0.86 ± 0.17 (0.60–1.22)[a]	0.662
Control group	0.88 ± 0.13 (0.72–1.24)[a]	0.8 ± 0.19 (0.32–1.33)[a]	0.81 ± 0.2 (0.19–1.03)[a]	0.920
P†	0.833	0.522	0.984	

Means with different letters ([a] or [b]) are significantly different ($P < 0.05$, Wilcoxon Signed Ranks Test for paired data with Bonferroni correction).
* P: By Friedman test.
† P: compared between ESWT group and control group by Mann–Whitney U-tests.

Table 4 – The mean autograft screw ratios, autograft integration ratios, and enlargement ratios of diameters and areas of the tibia tunnels on MR images for the patients in ESWT and control groups.

Ratios	ESWT group (mean ± SD)	Control group (mean ± SD)	P
Autograft screw ratio			
T0	4.03 ± 1.16	4.08 ± 0.92	0.652
T6 mo	1.28 ± 0.74	1.91 ± 0.75	0.002
T24 mo	0.60 ± 0.35	1.11 ± 0.32	<0.001
Autograft integration ratio			
T6 mo/T0	0.68 ± 0.15	0.51 ± 0.19	0.001
T24 mo/T0	0.85 ± 0.73	0.74 ± 0.08	<0.001
T24 mo/T6 mo	0.45 ± 0.19	0.39 ± 0.19	0.270
Tibia tunnel enlargement ratio			
AP diameter			
T6 mo/T0	1.12 ± 0.11	1.21 ± 0.13	0.018
T24 mo/T0	1.08 ± 0.26	1.25 ± 0.18	0.001
T24 mo/T6 mo	0.96 ± 0.17	1.03 ± 0.13	0.134
ML diameter			
T6 mo/T0	1.11 ± 0.11	1.19 ± 0.15	0.024
T24 mo/T0	0.98 ± 0.13	1.13 ± 0.13	<0.001
T24 mo/T6 mo	0.89 ± 0.10	0.95 ± 0.07	0.022
Area			
T6 mo/T0	1.25 ± 0.21	1.45 ± 0.29	0.008
T24 mo/T0	1.05 ± 0.30	1.42 ± 0.25	<0.001
T24 mo/T6 mo	0.86 ± 0.24	0.98 ± 0.14	0.006

T0, T6 mo, and T24 mo: 1 wk and 6 and 24 mo after treatment; Autograft screw ratio = mean autograft cross-sectional area/screw cross-sectional area; Integration ratio = 1 − (autograft screw ratio at T6 mo or T24 mo/autograft area ratio at T0 or T6 mo); Enlargement ratio = the value of diameter or area at T6 mo or T24 mo/the value of diameter or area at T0 or T6 mo; All P values are analyzed by Mann–Whitney U-tests.

However, no significant difference was demonstrated on the data between the T24 mo and T6 mo in both groups ($P = 0.270$). The enlargement ratios of diameters and areas of the tibia tunnel on MRI are also listed in the Table 4. Compared with the values at T0, all enlargement ratios at T6 mo and T24 mo in AP diameters, ML diameters, and areas in ESWT group were significantly lower than those in the control group (all $P < 0.05$). The enlargement ratio of the ML diameter and area in ESWT group at T24 mo/T6 mo appeared significantly lower than that in the control group ($P = 0.022$ and 0.006, respectively). Cyst formation or fluid collection in or around the tibia tunnel was not noticed in either group.

3.1. *Complications*

There were no systemic or local complications or ESWT device related problems. There were no infection, deep vein thrombosis, stiff knee, or neurovascular complications. Five cases in the ESWT group and seven cases in the control group showed quadriceps atrophy >2.0 cm, and the problems improved with outpatient physical therapy and home exercise. Six cases in the ESWT group and eight cases in the control group complained of donor site morbidity including local tenderness, itching and numbness, and all improved with conservative treatments. Graft failure as defined >5 mm anterior laxity was seen in one case at 1 y and three cases at 2 y in the control group, and none in the ESWT group.

4. Discussion

The results of the present study showed that the application of ESWT to the bone tunnel significantly improved the functional outcome and decreased the tibia tunnel enlargement after hamstring autograft ACL reconstruction compared with the control group. The healing of tendon to bone in a bone tunnel continues to be debated [2,4]. Many studies attempted to improve the healing between tendon and bone with different materials and methods. Some achieved limited success, but none showed consistent results [14–21]. Some authors reported that autograft ligamentization in the bone tunnel after ACL reconstruction was ascribed to ensuing vascularization of perigraft soft tissue with subsequent synovialization and remodeling [1,36]. Other studies reported that the maturation of the tendon–bone interface completed from 6 to 12 mo after ACL reconstruction [8,37]. Before autograft maturation has taken place, it is necessary that temporary fixation of the autograft for autograft protection after ACL reconstruction. Many factors may affect the outcome of ACL reconstruction including tunnel placement, fixation type, and autograft tension [9,28]. Prior studies showed that ESWT induces the ingrowth of neovascularization with upregulation of angiogenic growth factors, improves blood perfusion, and tissue regeneration [22,24]. It is reasonable to believe that the application of ESWT improves the outcome and decreases the bone tunnel enlargement after ACL reconstruction *via* the increases of vascularity and tissue regeneration.

In clinical setting, MRI is considered to be the best method in evaluation of the healing of tendon to bone at the tendon–bone interface after ACL reconstruction in human subjects [27–31]. The implication of bone tunnel enlargement after ACL reconstruction and subsequent mechanical instability is still debated [25–30]. Both radiograph and MRI can be used to evaluate the bone tunnel enlargement after ACL

surgery. However, MRI provides more precise information at the tendon–bone interface including the integration of the autograft, the contact and the gap, if any, between tendon and bone, the enlargement of bone tunnel, and the overall healing of tendon to bone. The functional outcomes after ACL reconstruction should be assessed in conjunction with clinical assessment, ligament stability, radiographs, and MRI studies. Better functional outcomes are parallel to the integrity of the autograft and healing of tendon to bone as shown on MRI. In our study, the ESWT group exhibited significantly smaller middle third of the tibia tunnel on X-ray at 2 y, and significantly less enlargement of the tibia tunnel in AP diameter, ML diameter, and area of the tibia tunnel on MRI. Several reports addressed that the tibia tunnel enlargement might play a pivotal role in the ultimate laxity of the autograft [25,29,30]. However, other studies reported no correlation between tibia tunnel enlargement, knee stability, joint function, and patient satisfaction scores after ACL reconstruction in short-term [26–28]. In this study, the ESWT-treated knees showed a better Lysholm score and AP laxity of the knee when compared with the control group. Furthermore, MRI exhibited significant decrease of tibia tunnel enlargement at 6 and 24 mo after treatment.

4.1. *Limitations*

There are limitations in this study. The follow-up time of this study was relatively short, and the functional results presented in this study may prove to be different in long-term follow-up. The evaluation of tendon–bone integration was based on radiograph and MRI evaluation, and no histologic examination of the biopsy specimen was used. MRI is considered to be the best method in the evaluation of the healing of tendon to bone at the tendon–bone interface after ACL reconstruction. MRI provides more precise information at the tendon–bone interface including the integration of the autograft, the contact, and the gap compared with X-ray examination. Nevertheless, the tendon–bone healing cannot be claimed without a biopsy. The integration of tendon graft to bone in bone tunnel may represent graft maturation rather than ligamentization with Sharpey fibers. The changes in the size of bone tunnel may be affected by many factors including drilling of the tunnel and fixation types. It is difficult to ascertain that the application of ESWT can affect the bone metabolism more than drilling of the bone tunnel. Furthermore, the dosage of EWST so chosen in this study was based on our previous experience, and the optimal dosage of EWST is unknown. Finally, the concomitant surgery for meniscus tear and chondral lesion may have impact on the functional outcome after ACL reconstruction.

5. Conclusions

Application of ESWT significantly improves the subjective Lysholm score and decreases middle 1/3 tibia tunnel enlargement after single hamstring autograft ACL reconstruction.

Acknowledgment

The authors acknowledge funding in total or in part for this research. The funding source was National Science Council (NSC96-2314-B-182A-143) and Chang Gung Research Fund (CMRPG8B1291).

Disclosure

The authors reported no proprietary or commercial interest in any product mentioned or concept discussed in this article.

REFERENCES

[1] Amiel D, Kleiner JB, Roux RD, Harwood FL, Akeson WH. The phenomenon of "ligamentization": anterior cruciate ligament reconstruction with autogenous patellar tendon. J Orthop Res 1986;4:162. PMID: 3712125.
[2] Arnoczky SP, Torzilli PA, Warren RF, Allen AA. Biologic fixation of ligament prosthesis and augmentations. An evaluation of bone ingrowth in the dog. Am J Sports Med 1988;16:106. PMID: 2967642.
[3] Bosch U, Kasperczyk W, Reinert C, Oestern HJ, Tscherne H. Healing at graft fixation site under functional conditions in posterior cruciate ligament reconstruction: a morphological study in sheep. Arch Orthop Trauma Surg 1989;108:154. PMID: 2730297.
[4] Bosch U, Kasperczyk WJ. Healing of the patellar tendon autograft after posterior cruciate ligament reconstruction – a process of ligamentization? An experimental study in a sheep model. Am J Sports Med 1992;20:558. PMID: 2730297.
[5] Forward AD, Cowan RJ. Tendon suture to bone: an experimental investigation in rabbits. J Bone Joint Surg Am 1963;45:807.
[6] Hausman M, Bain S, Ribin C. Reluctance of metaphyseal bone to heal to tendon: histologic evidence for poor mechanical strength. Trans Orthop Res Soc 1989;14:277.
[7] Kernwein G, Fahey J, Garrison M. The fate of tendon, fascia and elastic connective tissue transplanted into bone. Ann Surg 1938;108:285. PMID: 17857233.
[8] Rodeo SA, Arnoczky SP, Torzilli PA, Hidaka C, Warren RF. Tendon-healing in a bone tunnel. A biomechanical and histological study in the dog. J Bone Joint Surg Am 1993;75:1795. PMID: 8258550.
[9] Whiston TB, Walmsley R. Some observations on the reactions of bone and tendon after tunneling of bone and insertion of tendon. J Bone Joint Surg Br 1960;42:377. PMID: 13855359.
[10] Hashimoto Y, Yoshida G, Toyoda H, Takaoka K. Generation of tendon-to-bone interface "enthesis" with use of recombinant BMP-2 in a rabbit model. J Orthop Res 2007;25:1415. PMID: 17557323.
[11] Martinek V, Latterman C, Usas A, et al. Enhancement of tendon-bone integration of anterior cruciate ligament grafts with bone morphogenetic protein-2 gene transfer: a histological and biomechanical study. J Bone Joint Surg Am 2002;84:1123. PMID: 12107310.
[12] Reddi AH. Role of morphogenetic proteins in skeletal tissue engineering and regeneration. Nat Biotechnol 1998;16:247. PMID: 9528003.
[13] Rodeo SA, Suzuki K, Deng XH, Wozney J, Warren RF. Use of recombinant human bone morphogenetic protein-2 to

enhance tendon healing in a bone tunnel. Am J Sports Med 1999;27:476. PMID: 10424218.
[14] Chen CH, Chen WJ, Shih CH, Yang CY, Liu SJ, Lin PY. Enveloping the tendon graft with periosteum to enhance tendon-bone healing in a bone tunnel: a biomechanical and histologic study in rabbits. Arthroscopy 2003;19:290. PMID: 12627154.
[15] Gulotta LV, Kovacevic D, Ying L, Ehteshami JR, Montgomery S, Rodeo SA. Augmentation of tendon-to-bone healing with a magnesium-based bone adhesive. Am J Sports Med 2008;36:1290. PMID: 18319348.
[16] Huangfu X, Zhao J. Tendon-bone healing enhancement using injectable tricalcium phosphate in a dog anterior cruciate ligament reconstruction model. Arthroscopy 2007;23:455. PMID: 17478274.
[17] Kyung HS, Kim SY, Oh CW, Kim SJ. Tendon-to-bone tunnel healing in a rabbit model: the effect of periosteum augmentation at the tendon-to-bone interface. Knee Surg Sports Traumatol Arthrosc 2003;11:9. PMID: 12548445.
[18] Lattermann C, Zelle BA, Whalen JD, et al. Gene transfer to the tendon-bone insertion site. Knee Surg Sports Traumatol Arthrosc 2004;12:510. PMID: 15014945.
[19] Mutsuzaki H, Sakane M, Nakajima H, et al. Calcium-phosphate-hybridized tendon directly promotes regeneration of tendon-bone insertion. J Biomed Mater Res A 2004;70:319. PMID: 15227677.
[20] Sasaki K, Kuroda R, Ishida K, et al. Enhancement of tendon-bone osteointegration of anterior cruciate ligament graft using granulocyte colony-stimulating factor. Am J Sports Med 2008;36:1519. PMID: 18413678.
[21] Tien YC, Chih TT, Lin JH, Ju CP, Lin SD. Augmentation of tendon-bone healing by the use of calcium-phosphate cement. J Bone Joint Surg Br 2004;86:1072. PMID: 15446542.
[22] Wang CJ, Huang HY, Pai CH. Shock wave-enhanced neovascularization at the tendon-bone junction: an experiment in dogs. J Foot Ankle Surg 2002;41:16. PMID: 11858601.
[23] Wang CJ, Wang FS, Yang KD, Weng LH, Sun YC, Ko YJ. The effect of shock wave treatment at the tendon-bone interface: an histomorphological and biomechanical study in rabbits. J Orthop Res 2005;23:274. PMID: 15734237.
[24] Wang CJ, Wang FS, Yang KD, et al. Shock wave therapy induces neovascularization at the tendon-bone junction. A study in rabbits. J Orthop Res 2003;21:984. PMID: 14554209.
[25] Järvelä T, Moisala AS, Paakkala T, Paakkala A. Tunnel enlargement after double-bundle anterior cruciate ligament reconstruction: a prospective, randomized study. Arthroscopy 2008;24:1349. PMID: 19038705.
[26] Buelow JU, Siebold R, Ellermann A. A prospective evaluation of tunnel enlargement in anterior cruciate ligament reconstruction with hamstrings: extracortical versus anatomical fixation. Knee Surg Sports Traumatol Arthrosc 2002;10:80. PMID: 11914764.
[27] Fules PJ, Madhav RT, Goddard RK, Newman-Sanders A, Mowbray MA. Evaluation of tibia bone tunnel enlargement using MRI scan cross-sectional area measurement after autologous hamstring tendon ACL replacement. Knee 2003; 10:87. PMID: 12649033.
[28] Jansson KA, Harilainen A, Sandelin J, Karjalainen PT, Aronen HJ, Tallroth K. Bone tunnel enlargement after anterior cruciate ligament reconstruction with the hamstring autograft and endobutton fixation technique. A clinical, radiographic and magnetic resonance imaging study with 2 years follow-up. Knee Surg Sports Traumatol Arthrosc 1999;7:290. PMID: 10525698.
[29] Moisala AS, Järvelä T, Paakkala A, Paakkala T, Kannus P, Järvinen M. Comparison of the bioabsorbable and metal screw fixation after ACL reconstruction with a hamstring autograft in MRI and clinical outcome: a prospective randomized study. Knee Surg Sports Traumatol Arthrosc 2008;16:1080. PMID: 18762911.
[30] Singhal MC, Holzhauer M, Powell D, Johnson DL. MRI evaluation of the tibia tunnel/screw/tendon interface after ACL reconstruction using a bioabsorbable interference screw. Orthopedics 2008;31:575. PMID: 18661880.
[31] Paessler HH, Mastrokalos DS. Anterior cruciate ligament reconstruction using semitendinosus and gracilis tendons, bone patellar tendon, or quadriceps tendon-graft with press-fit fixation without hardware. A new and innovative procedure. Orthop Clin North Am 2003;34:49. PMID: 12735201.
[32] Barber FA, Dockery WD, Hrnack SA. Long-term degradation of a poly-lactide co-glycolide/β-tricalcium phosphate biocomposite interference screw. Arthroscopy 2011;27:637. PMID: 21429700.
[33] Brucker PU, Lorenz S, Imhoff AB. Aperture fixation in arthroscopic anterior cruciate ligament double-bundle reconstruction. Arthroscopy 2006;22:1250.e1. PMID: 17084308.
[34] Hu J, Qu J, Xu D, Zhou J, Lu H. Allograft versus autograft for anterior cruciate ligament reconstruction: an up-to-date meta-analysis of prospective studies. [Review] Int Orthopaedics 2013;37:311. PMID: 23207581.
[35] Wang CJ, Yang KD, Wang FS, Hsu CC, Chen HH. Shock wave treatment shows dose-dependent enhancement of bone mass and bone strength after fracture of the femur. Bone 2004;34:225. PMID: 14751581.
[36] Jansson KA, Karjalainen PT, Harilainen A, et al. MRI of anterior cruciate ligament repair with patellar and hamstring tendon autografts. Skeletal Radiol 2001;30:8. PMID: 11289638.
[37] Murakami Y, Sumen Y, Ochi M, Fujimoto E, Deie M, Ikuta Y. Appearance of anterior cruciate ligament autografts in their tibial bone tunnels on oblique axial MRI. Magn Reson Imaging 1999;17:679. PMID: 10372521.